IJAME

Int. J. of Applied Mechanics and Engineering, 2025, vol.30, No.1, pp.1-20
DOI: 10.59441/ijame/199646

EDDY CURRENT LOSS BEHAVIOR OF HOLLOW CIRCULAR CYLINDER DUE TO TIME-VARYING ELECTROMAGNETIC FIELD

B.B. Balpande and G.D. Kedar*
Department of Mathematics, RTM Nagpur University, Nagpur-440033, Maharashtra, INDIA
E-mail: gdkedar@rediffmail.com

J.L. Matlam
Department of Mathematics, J.M. Patel Arts, Commerce & Science College,
Bhandara-441904, Maharashtra, INDIA

The purpose of this study is to investigate the effects of a time-varying electromagnetic field on the quasi-static thermoelastic behavior of a finitely conducting hollow circular cylinder. As a consequence of a time-varying electromagnetic field, conducting currents, also known as eddy currents, are induced inside the cylinder. We treat the Joule heat that the induced eddy currents generate due to resistive heating as a thermal loading of the cylinder. The cylinder thickness is considered negligible in comparison to the magnetic field's penetration depth, and the problem is considered one-dimensional. The convection-type boundary conditions are applied across the curved surface of the cylinder. The intensity of Joule heat in terms of current density and eddy current loss is obtained in quasi-static form using integral transform techniques, which include the finite Hankel transform, the Marchi Zgrablich transform, and the Laplace transform. The quasi-static solutions of thermal stresses, displacement, non-dimensional temperature, eddy current loss, and magnetic field fluctuations are obtained in terms of electrical conductivity, magnetic permeability, frequency, and magnetic intensity of the electromagnetic field applied and are illustrated graphically using MATLAB software.

Key words: Joule heat, eddy current loss, skin effect, magneto-thermoelasticity, finite Hankel and Laplace transform, Marchi-Zgrablich transform.

1. Introduction

Whenever the current passes through an electrical conductor, it produces thermal energy. This physical effect is known as joule heating. This thermal energy raises the conductive material's temperature. Joule heating is the transformation between electrical and thermal energy based on the principle of energy conservation. Around 1840, the famous amateur scientist James Prescott Joule was the first to observe and study the heating effect. He found that the recently invented electrical motor could be more useful than the steam engines in use at the process in terms of cost and efficiency. He found that the newly invented electric motors could be more advantageous in terms of cost and efficiency than the steam engines, which were used earlier in various processes. According to the law of conservation of energy, for an isolated system, the total energy is always conserved over time. To put it another way, we cannot create or destroy energy; instead, it continuously transforms into different forms. Therefore, “losses” is an incorrect or unsuitable word. Electrical devices and electromagnetic circuits permit the transfer of energy from one source to the other. But all this input energy is ultimately not used for its intended purpose. Some amount of energy is lost, mostly in the form of heat.

With the rapid advancement in the field of electromechanics, many devices, including magnetic circuits of electric motors, inductors, transformers, and generators that operate under the impact of changes in electromagnetic fields and get activated owing to these fluctuations, play key roles in modern technology. In recent years, significant attention has been observed in the field of so-called high-frequency heating, also known

* To whom correspondence should be addressed

as induction heating. It operates on the electromagnetic induction principle. During high-frequency heating, close-loop (eddy) currents are created inside the body. This is a type of contactless heating technique for conductive bodies. The electrical resistance of the body material produces a heating effect. Due to this heating effect, excess heat is generated that remains unused; we call this unused heat an eddy current loss. The elastic components and structures exposed to mechanical loads caused by a highly fluctuating magnetic field generate several forms of stress. In addition to mechanical stress, they also generate magnetic stress caused by the Lorentz force and thermal stress caused by induced eddy currents. Electromagnetic induction occurs when a magnetic field is applied to a conductor that is carrying an electric current, leading to the generation of eddy currents. Due to the wide range of applications of electromagnetic structures in the various diversified fields, the study of electromagnetic coupling's thermos-elastic phenomenon has a solid theoretical foundation in engineering [1-3].

In the emerging topic of thermo-magneto-elasticity, we examine the stability, stiffness, and strength of various electromagnetic device components that operate under the combined influence of temperature, deformation, and electromagnetic fields. Thermo-elasticity is the examination of the relationship between temperature and elasticity, specifically focusing on the interaction between the temperature field and the elastic field. In contrast, magnetoelasticity studies electromagnetic forces and deformation. Heat conduction theory, electromagnetic theory, and classical elasticity theory are all included in thermo-magneto-elasticity. These theories are used to address the coupling issues between the thermal effect and the electromagnetic, temperature, and elastic fields of conductive materials placed in time-varying or steady magnetic fields. Wang [4] presented an effective method for the determination of the distribution of the dynamic thermoelastic stress in a hollow cylinder that is subjected to rapid arbitrary heating. Xing and Liu [5] used the difference method to study the quasi-static and dynamic responses of a rectangular plate in a magnetic field that varied in temperature. Using a variable separation method, Higuchi *et al.* [6-7] investigated the effect of changes in magnetic field and thermo-magneto-elastic stresses on a hollow cylindrical shell. The investigation of thermal stresses coming from eddy current loss and magnetic stresses arising from Lorentz force in a conducting half space created by an imposed rise through the tangential magnetic field along the boundary has been carried out by Moon and Chattopadhyay [8]. The aforementioned work has been expanded upon by Chian and Moon [9], who examined the stresses induced by a pulsed magnetic field at the cavity in a cylindrical conductor. Wauer [10] investigated the dynamic characteristics of a magneto-thermo-elastic plate layer subjected to a magnetic field comprising a sinusoidally fluctuating component parallel to the surfaces and a constant component. Pantelyat and Fe´liachi [11] examined the mechanical properties of metals in induction heating systems using the finite element approach. They calculated the thermo-elastic-plastic stresses induced by an alternating magnetic field using the material's temperature-dependent characteristics. A model was created by Sinha and Prabhu [12] to investigate the eddy current that is created in thin nonmagnetic plates when they are subjected to fluctuating magnetic fields over time. Xu and Cen [13] studied the dynamic reaction of a shallow conical shell's thermos-magneto-elastic behavior in a magnetic field that changes with time. Plotnikov [14] studied the problem of separation of the total losses in the electric steel of a magnetic circuit in terms of hysteresis loss and eddy current loss and discussed the frequency dependence of both losses in steel material. Ekergård and Leijon [15] investigated the eddy current losses in the rotor of a two-pole permanent magnet motor using three different analytical models. Wang *et al.* [16] analyzed the eddy current loss characteristics of magnetic couplings using two-dimensional finite element simulation and experiment.

Golebiowski [17] developed a method for calculating the eddy current loss and hysteresis loss in laminated magnetic circuits. Also, the nonlinear magnetization characteristic of iron in the simulations done with the developed method. Kumar and Kamdi [18] analyzed the thermal behavior of a finite hollow cylinder using the theory of fractional thermoelasticity due to convection-type boundary conditions. Lamba [19] explored the memory-dependent thermoelastic response of a cylindrical solid object with radiation-like boundary conditions. Using the integral transform technique, Srinivas *et al.* [20] investigated the effect of point heating on temperature variation in multilayered annular circular discs. Biswas [21] introduced magneto-thermoelastic interaction using a three-phase-lag model of generalized thermoelasticity, adopting the eigenfunction expansion approach. Gao *et al.* [22] investigated and compared the eddy current pulsed thermography configurations for the analysis of metallic materials and defects with the traditional line-coil configuration. Li *et al.* [23] introduced a novel approach to the quantitative study of the damage characteristics

for the fiber texture of a CFRP-steel structure using transient thermal images. Lotfy *et al.* [24] studied a one-dimensional fractional model of a spherical, tiny semiconductor cavity in the presence of a magnetic field and initial stresses. Abo-Dahab and Lotfy [25] determined the displacements, stresses, and temperature distributions in a rotating fiber-reinforced generalized thermoelastic medium using normal mode analysis. Using normal mode analysis, Lotfy [26] investigated a two-dimensional problem of infinite space weakened by mode-I crack. Lotfy and Tantawi [27] describe a one-dimensional model of generalized thermoelasticity theory in the context of the photothermal transport process of functionally graded material in the presence of the initial constant magnetic field. Abo-Dahab *et al.* [28] examined the surface wave propagation at an imperfect boundary between an isotropic elastic layer and isotropic thermodiffusive elastic half-space with rotation in the context of Green-Lindsay theory.

In the present work, we have studied and analyzed the eddy current loss behavior of hollow circular cylinders and the fallout from it. The problem is mathematically described using Maxwell's equations, and the partial differential equation of the magnetic field along with the suitable boundary conditions are obtained. The cylinder is assumed to be at zero initial temperature and then gradually heats up due to the consequence of Joule heat generated inside the cylinder. It is also assumed that the conducting hollow cylinder is nonmagnetic, and the thickness is considered to be minimal as compared to other parameters of the cylinder. One of the most suitable integral transforms for convection-type boundary conditions is the Marchi-Zgrablich integral transform, and its inversion is used for numerical calculation. The results are obtained theoretically using the integral transform techniques [29-33] and have been computed numerically. Eddy current's impact on temperature, displacement, thermal, and magnetic stresses are then illustrated graphically using MATLAB software for the case of the time-varying magnetic field as a function of sine function.

2. Formulation of the problem

Let us assume that a non-magnetic finite hollow circular cylinder with inner and outer radii as a and b respectively, as shown in Fig.1, is subjected to a time-varying axial magnetic field starting at time $t = 0$. This magnetic field is assumed to have an arbitrary time history and is expressed as $H_0\varphi(t)$. Let the components of the magnetic field for the conducting cylinder be $(0,0,H_z(r,t))$.

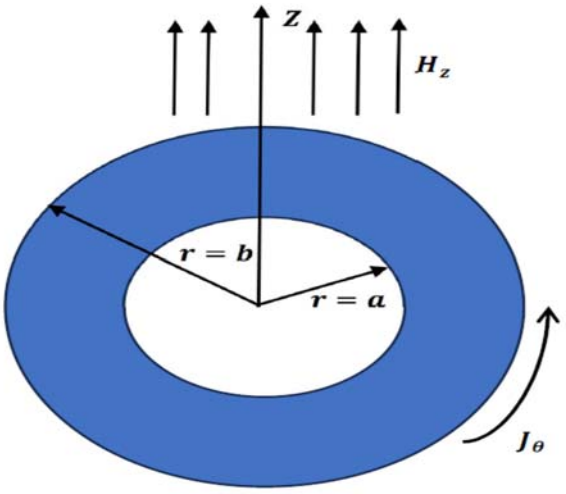

Fig.1. Geometry of the problem.

Setting aside the displacement current and charge density, the set of Maxwell's equations and constitutive relations for a homogeneous, isotropic conducting cylinder in terms of the cylindrical coordinate system (r,θ,z), can be written as:

$$\vec{\nabla}\times\vec{E}=-\frac{\partial\vec{B}}{\partial t}, \tag{2.1}$$

$$\vec{\nabla}\times\vec{H}=\vec{J}, \tag{2.2}$$

$$\vec{J}=\sigma\vec{E}, \tag{2.3}$$

$$\vec{B}=\mu_e\vec{H}, \tag{2.4}$$

where $\vec{\nabla}$ is the Hamilton's operator, $\vec{B}$, $\vec{H}$ and $\vec{E}$ are the magnetic induction intensity, magnetic field intensity, and electric field intensity in the conducting cylinder, respectively; σ is the electrical conductivity; and μ_e is the magnetic permeability.

The axial component of the magnetic flux can be obtained from Eq.(2.4), as:

$$B_z=\mu_e H_z(r,t). \tag{2.5}$$

The component of the induced electric field of the conducting cylinder is obtained from Eqs (2.1) and (2.2) as:

$$\vec{E}=(0,E_{\theta,}0)=\left(0,-\frac{1}{\sigma}\frac{\partial H_z}{\partial r},0\right). \tag{2.6}$$

From Eqs (2.2) and (2.3), the current density components are obtained and read as:

$$\vec{J}=(0,J_{\theta,}0)=(0,\sigma E_{\theta,}0)=\left(0,-\frac{\partial H_z}{\partial r},0\right). \tag{2.7}$$

For the considered problem, it is assumed that all the field variables are functions of the radial coordinate r and time t solely. This is because the axis of the cylinder and the z-axis are overlapping, as shown in the figure.

Due to the cylindrical symmetry of the problem, the component of displacement is a function of radial coordinate only and is read as:

$$u_r=u(r,t), u_\theta=u_z=0. \tag{2.8}$$

The considered problem will be treated as one-dimensional, in which all the field variables are independent of θ and z. To determine the fundamental equation of the magnetic field, we solve Eqs (2.1) and (2.2) together with Eqs (2.5) and (2.6) and obtain:

$$r\frac{\partial^2 H_z}{\partial r^2}+\frac{\partial H_z}{\partial r}=-\sigma\mu_e r\frac{\partial H_z}{\partial t}. \tag{2.9}$$

The prescribed boundary and initial conditions are:

$$H_z(b,t)=H_0\varphi(t), \tag{2.10}$$

$$H_z(b,0)=0. \tag{2.11}$$

Eddy current is another name for the electric current density $\vec{J}$ caused by the temporal fluctuation of the magnetic field. This current density generates joule heat, known as the "eddy current loss." It is denoted by $w(r,t)$ and is provided by [7]:

$$w(r,t)=\frac{\left[J_{\theta}(r,t)\right]^{2}}{\sigma}. \tag{2.12}$$

We assume that starting at time $t=0,$ the eddy current loss $w(r,t)$ heats the hollow cylinder, which started at zero initial temperature. The basic equation of heat conduction, which accounts for eddy current loss, along with the boundary and initial conditions, is read as:

$$\kappa\frac{1}{r}\frac{\partial}{\partial r}\left(r\frac{\partial T}{\partial r}\right)+\frac{w}{C\rho}=\frac{\partial T}{\partial t}, \tag{2.13}$$

where κ, C denotes thermal conductivity and specific heat of hollow cylinder.
We assume that the cylinder is at rest initially, therefore the initial boundary conditions are:

$$(u)_{t=0}=\left(\frac{\partial u}{\partial t}\right)_{t=0}=(T)_{t=0}=0. \tag{2.14}$$

The boundary conditions are assumed to be of the following form:

(1) Thermal boundary conditions:

$$\left(T-\frac{1}{h_a}\frac{\partial T}{\partial r}\right)_{r=a}=0, \tag{2.15}$$

$$\left(T+\frac{1}{h_b}\frac{\partial T}{\partial r}\right)_{r=b}=0. \tag{2.16}$$

(2) Mechanical boundary conditions:

$$\left(\frac{\partial u_r}{\partial r}+\frac{\nu}{1-\nu}\frac{u_r}{r}\right)_{r=a,b}=\left(\frac{1+\nu}{1-\nu}\right)\alpha T. \tag{2.17}$$

Here the heat transfer coefficients at the inner and outer radii are expressed as h_a and h_b respectively.
The time-varying electromagnetic field and temperature stress caused by Lorentz force and Joule heat are experienced by the hollow cylinder and are determined by [13]:

$$\vec{F}=\mu_e(\vec{J}\times\vec{B}), \tag{2.18}$$

where $\vec{J}$ denotes the current density vector. The Lorentz force components are obtained by using Eqs (2.3) and (2.4) and are written as:

$$\vec{F}=(f_r,0,0)=\left(-\frac{\mu_e}{2}\frac{\partial}{\partial r}\left[H_z\right]^2,0,0\right). \tag{2.19}$$

In the context of magneto-thermoelasticity, the equation of motion taking into account the Lorentz force in the radial direction is given by:

$$\frac{\partial \sigma_{rr}}{\partial r}+\frac{\sigma_{rr}-\sigma_{\theta\theta}}{r}+f_r=\rho\frac{\partial^2 u}{\partial t^2}, \tag{2.20}$$

where f_r is the Lorentz force component and ρ is the mass density.
The stress-displacement relations accounting for temperature variation due to conducting currents can be expressed by the following relations:

$$\sigma_{rr}=(2\mu+\lambda)\frac{\partial u_r}{\partial r}+\lambda\frac{u_r}{r}-\beta T, \tag{2.21}$$

$$\sigma_{\theta\theta}=(2\mu+\lambda)\frac{u_r}{r}+\lambda\frac{\partial u_r}{\partial r}-\beta T, \tag{2.22}$$

$$\sigma_{zz}=(2\mu+\lambda)\frac{\partial u_z}{\partial z}+\lambda\left[\frac{\partial u_r}{\partial r}\frac{u_r}{r}\right]-\beta T, \tag{2.23}$$

where σ_{zz} is the stress component along the axis of the cylinder, $\sigma_{\theta\theta}$ is the circumferential stress, T is the cylinder's temperature, and β represents the thermal moduli. For the one-dimensional symmetric case taken into consideration, the strain components are expressed as:

$$e_{rr}=\frac{\partial u_r}{\partial r},\quad e_{\theta\theta}=\frac{u_r}{r},\quad e_{zz}=e_{rz}=e_{r\theta}=e_{\theta z}=0, \tag{2.24}$$

$$e=e_{rr}+e_{\theta\theta}+e_{zz}=\frac{\partial u_r}{\partial r}+\frac{u_r}{r}=\frac{1}{r}\frac{\partial(ru_r)}{\partial r}, \tag{2.25}$$

$$\frac{\partial e}{\partial r}=\frac{\partial}{\partial r}\left(\frac{\partial u_r}{\partial r}+\frac{u_r}{r}\right)=\frac{\partial^2 u_r}{\partial r^2}+\frac{1}{r}\frac{\partial u_r}{\partial r}-\frac{u_r}{r^2}. \tag{2.26}$$

Using Eqs (2.21-2.23) in Eq.(2.20), the displacement equation of motion can be found as:

$$\frac{\partial^2 u_r}{\partial r^2}+\frac{1}{r}\frac{\partial u_r}{\partial r}-\frac{1}{r^2}u_r=\frac{\rho}{(2\mu+\lambda)}\frac{\partial^2 u_r}{\partial t^2}+\frac{\beta}{(2\mu+\lambda)}\frac{\partial T}{\partial r}+\frac{1}{(2\mu+\lambda)}\frac{\mu}{2}\frac{\partial}{\partial r}(H_z)^2. \tag{2.27}$$

Dimensionless variables in the governing equations are always important for theoretical and computational purposes. A dimensionless variable is characterized as a ratio between two physical quantities that describes the system and the behavior of the system without units of measurement. Using dimensionless variables is advantageous as it reduces the amount of experimental data by reducing the number of variables that describe the system. The dimensionless variables used in the present work are:

$$\bar{r}=\frac{r}{a},\quad \bar{a}=\frac{a}{b},\quad \bar{H}_z=\frac{H_z}{H_0},\quad \tau=\frac{t}{\mu_e\sigma b^2},\quad \bar{J}_\theta=\frac{bJ_\theta}{H_0},\quad \bar{w}=\frac{\sigma b^2 w}{H_0^2},\quad \bar{T}=\frac{C\gamma T}{\mu_e H_0^2}, \tag{2.28}$$

$$\bar{f}_r = \frac{bf_r}{\mu_e H_0^2}, \quad (\bar{\sigma}_{rr}, \bar{\sigma}_{\theta\theta}, \bar{\sigma}_{zz}) = \left(\frac{2}{\mu_e H_0^2}\sigma_{rr}, \frac{2}{\mu_e H_0^2}\sigma_{\theta\theta}, \frac{2}{\mu_e H_0^2}\sigma_{zz} \right),$$

$$(\bar{h}_a, \bar{h}_b) = (bh_a, bh_b), \quad \bar{u}_r = \frac{(1-\nu)E}{(1+\nu)(1-2\nu)} \frac{2}{b\mu_e H_0^2} u_r. \tag{2.28 cont}$$

Using the above dimensionless variables, the electromagnetic field Eqs (2.9-2.11) are modified and expressed in dimensionless form as:

$$a\bar{r} \frac{\partial^2 \bar{H}_z}{\partial \bar{r}^2} + \frac{\partial \bar{H}_z}{\partial \bar{r}} = -\bar{r}\, \bar{a}^2 \frac{\partial \bar{H}_z}{\partial \tau}, \tag{2.29}$$

$$\left[\bar{H}_z(\bar{r}, \tau) \right]_{\bar{r}=\bar{a},\bar{b}} = \varphi(\tau), \tag{2.30}$$

$$\left[\bar{H}_z(\bar{r}, \tau) \right]_{\tau=0} = 0. \tag{2.31}$$

The dimensionless current density and eddy current loss are expressed as:

$$\bar{J}_\theta(\bar{r}, \tau) = -\frac{1}{\bar{a}} \frac{\partial \bar{H}_z}{\partial \bar{r}}, \tag{2.32}$$

$$\bar{w}(\bar{r}, \tau) = \left[\bar{J}_\theta(\bar{r}, \tau) \right]^2. \tag{2.33}$$

The dimensionless temperature field, along with the boundary and initial conditions, is read as:

$$\kappa \left[\frac{1}{\bar{r}} \frac{\partial \bar{T}}{\partial \bar{r}} + \frac{\partial^2 T}{\partial r^2} \right] + \chi_1 \bar{w} = \chi_2 \frac{\partial \bar{T}}{\partial t}, \tag{2.34}$$

$$\left(\bar{T} - \frac{1}{h_a} \frac{\partial \bar{T}}{\partial \bar{r}} \right)_{\bar{r}=1} = 0, \tag{2.35}$$

$$\left(T + \frac{1}{h_b} \frac{\partial \bar{T}}{\partial \bar{r}} \right)_{\bar{r}=\bar{a}} = 0, \tag{2.36}$$

$$\left[\bar{T}(\bar{r}, \tau) \right]_{\tau=0} = 0, \tag{2.37}$$

where $\chi_1 = \dfrac{\bar{a}^2 \gamma}{\sigma \rho \mu_e}, \quad \chi_2 = \dfrac{a^2 \gamma}{\sigma \mu_e b^2}.$

The dimensionless Lorentz force and stress and displacement components and dimensionless displacement equation are expressed as:

$$\bar{f}_r(\bar{r}, \tau) = -\frac{1}{2} \frac{\partial}{\partial \bar{r}} \left[\bar{H}_z(\bar{r}, \tau) \right]^2, \tag{2.38}$$

$$\bar{\sigma}_{rr}(\bar{r},\tau)=\frac{\partial \bar{u}_r}{\partial \bar{r}}+\frac{\nu}{1-\nu}\frac{\bar{u}_r}{\bar{r}}-\chi_3\bar{T}, \tag{2.39}$$

$$\bar{\sigma}_{\theta\theta}(\bar{r},\tau)=\frac{\bar{u}_r}{\bar{r}}+\lambda\frac{\partial \bar{u}_r}{\partial \bar{r}}-\chi_3\bar{T}, \tag{2.40}$$

$$\bar{\sigma}_{zz}(\bar{r},\tau)=\frac{\nu}{1-\nu}\left[\frac{\partial \bar{u}_r}{\partial \bar{r}}+\frac{\bar{u}_r}{\bar{r}}\right]-\chi_3\bar{T}, \tag{2.41}$$

$$\frac{\partial^2 \bar{u}_r}{\partial \bar{r}^2}+\frac{1}{\bar{r}}\frac{\partial \bar{u}_r}{\partial \bar{r}}-\frac{1}{\bar{r}^2}\bar{u}_r=\frac{1}{\chi_2^2}\frac{\partial^2 \bar{u}_r}{\partial \tau^2}+\chi_3\frac{\partial \bar{T}}{\partial \bar{r}}+\frac{\partial}{\partial \bar{r}}(\bar{H}_z)^2, \tag{2.42}$$

$$\left(\frac{\partial \bar{u}_r}{\partial \bar{r}}+\frac{\nu}{1-\nu}\frac{\bar{u}_r}{\bar{r}}\right)_{\bar{r}=1,\bar{a}}=\chi_3\bar{T}, \tag{2.43}$$

$$(\bar{u})_{\tau=0}=\left(\frac{\partial \bar{u}_r}{\partial \tau}\right)_{\tau=0}=0. \tag{2.44}$$

3. Integral transforms required for calculation

3.1. Marchi-Zgrablich integral transform (MZT)

Marchi-Zgrablich integral transform is one of the finite integral transforms, whose kernel is framed using the cylindrical functions and is used to solve the problems of heat conduction of circular cylinders with convective type boundary conditions on outer and inner surfaces. The finite Marchi-Zgrablich integral transform of order p over the variable r for $f(r)$ in $a \le r \le b$ is defined as [29]:

$$\bar{f}_p(m)=\int_a^b rf(r)S_p(\alpha,\beta,\mu_m r)dr, \tag{3.1}$$

along with the prerequisite boundary conditions:

$$\alpha_1 f(r)+\left[\alpha_2 f'(r)\right]_{r=a}=0, \tag{3.2}$$

$$\beta_1 f(r)+\left[\beta_2 f'(r)\right]_{r=b}=0, \tag{3.3}$$

where α_1 and α_2,β_1,β_2 are the constants involved in the above boundary conditions:
For the differential equation,

$$f''(r)+\left(\frac{1}{r}\right)f'(r)-\left(\frac{p^2}{r^2}\right)f(r)=0, \tag{3.4}$$

the finite Marchi-Zgrablich integral transform is given by:

$$\int_a^b \left[f''(r) + \left(\frac{1}{r}\right) f'(r) - \left(\frac{p^2}{r^2}\right) f(r) \right] S_p(\alpha,\beta,\mu_m r)\, dr = \\ = \frac{b}{\beta} S_p(\alpha,\beta,\mu_m b)\left[f(r) + \beta f'(r) \right]_{r=b} - \frac{a}{\alpha} S_p(\alpha,\beta,\mu_m a)\left[f(r) + \alpha f'(r) \right]_{r=a} - \mu_m^2 \bar{f}_p(m). \tag{3.5}$$

The inversion of Eq.(3.1) is given by:

$$f(r) = \sum_{m=1}^{\infty} \frac{\bar{f}_p(m) S_p(\alpha,\beta,\mu_m r)}{\int_a^b \left[r S_p(\alpha,\beta,\mu_m r) \right]^2 dr}, \tag{3.6}$$

where the kernel function $S_p(\alpha,\beta,\mu_m r)$ can be defined as:

$$S_p(\alpha,\beta,\mu_m r) = J_p(\mu_m r)\left[Y_p(\alpha,\mu_m a) + Y_p(\beta,\mu_m b) \right] - Y_p(\mu_m r)\left[J_p(\alpha,\mu_m a) + J_p(\beta,\mu_m b) \right], \tag{3.7}$$

and $J_p(\mu r)$ and $Y_p(\mu r)$ are Bessel's function of the first and second kind respectively.

3.2. Finite Hankel transform

The most appropriate integral transform for solving boundary value problems with axial symmetry, which naturally comes in the problems framed in cylindrical coordinates, is the finite Hankel transform. In 1946, Sneddon [33] was the first to introduce the transform and used it for solving boundary value problems with axial symmetry.
The finite Hankel transform for the variable r considered in an interval (a,b) is given by [30]:

$$\mathrm{H}\{f(r)\} = \int_a^b r f(r)\left[J_\mu(\xi_i r) G_\mu(\xi_i b) - G_\mu(\xi_i r) J_\mu(\xi_i b) \right] dr = \bar{f}_\mathrm{H}(\xi_i), \tag{3.8}$$

where $b > a$ and G_μ is the Bessel function of the second kind defined by the equation:

$$G_\mu(z) = \frac{1}{2}\pi \cos ec\, \mu z \left\{ J_{-\mu}(z) - e^{i\mu\pi} J_\mu(z) \right\}. \tag{3.9}$$

The appropriate inversion formula is given by:

$$f(r) = \mathrm{H}^{-1}\left[\bar{f}_\mathrm{H}(\xi_i) \right] = \sum_i 2\xi_i^2 \frac{\bar{f}_\mathrm{H}(\xi_i) J_\mu^2(\xi_i b)}{J_\mu^2(\xi_i a) - J_\mu^2(\xi_i b)} \left\{ J_\mu(\xi_i r) G_\mu(\xi_i a) - G_\mu(\xi_i r) J_\mu(\xi_i a) \right\}. \tag{3.10}$$

The sum in the above equation is taken over all the positive roots of the equation:

$$J_\mu(\xi_i b) G_\mu(\xi_i a) - G_\mu(\xi_i b) J_\mu(\xi_i a) = 0. \tag{3.11}$$

The finite Hankel transform defined in (3.8) satisfies the relation:

$$\mathrm{H}_{\mu}\left\{\frac{\partial^2 f}{\partial r^2}+\frac{1}{r}\frac{\partial f}{\partial r}-\frac{\mu^2}{r^2}\right\}=-\xi_i^2\mathrm{H}_{\mu}(f)+\left[\frac{a}{b}f(a)-f(b)\right]\frac{J_{\mu}(\xi_i a)}{J_{\mu}(\xi_i b)}. \tag{3.12}$$

4. Solutions

4.1. Magnetic field

The inhomogeneous boundary condition in Eqs (2.30) and (2.31) must first be converted into a homogeneous one to compute the magnetic field expression. To do this, we add a new function:

$$\Upsilon(\bar{r},\tau)=\bar{H}_z(\bar{r},\tau)-h_z(\bar{r},\tau), \tag{4.1}$$

where

$$h_z(\bar{r},\tau)=\varphi(\tau). \tag{4.2}$$

Using Eqs (3.1-3.3) in Eqs (2.29) and (2.31), we obtain:

$$\frac{\partial^2\Upsilon}{\partial\bar{r}^2}+\frac{\partial\Upsilon}{\partial\bar{r}}+\bar{a}^2\omega\cos\omega\tau=-\bar{a}^2\frac{\partial\Upsilon}{\partial\tau}, \tag{4.3}$$

$$\left[\Upsilon(\bar{r},\tau)\right]_{\bar{r}=\bar{a},\bar{b}}=0, \tag{4.4}$$

$$\left[\Upsilon(\bar{r},\tau)\right]_{\tau=0}=0. \tag{4.5}$$

To solve Eq.(4.3), we apply finite Hankel transform and obtain:

$$\beta_m^2\bar{\Upsilon}(\beta_m,\tau)+\frac{\bar{a}^2(b^2-a^2)}{2}\omega\cos\omega\tau K_0(\beta_m,\bar{r})=-\bar{a}^2\frac{\partial\bar{\Upsilon}(\beta_m,\tau)}{\partial\tau}, \tag{4.6}$$

where

$$K_0(\beta_m,\bar{r})=\frac{R_0(\beta_m,\bar{r})}{\sqrt{N}}, \tag{4.7}$$

$$R_0(\beta_m,\bar{r})=\frac{J_0(\beta_m\bar{r})}{J_0(\beta_m b)}-\frac{Y_0(\beta_m\bar{r})}{Y_0(\beta_m b)}, \tag{4.8}$$

$$N=\frac{b^2}{2}R_0'^2(\beta_m b)-\frac{a^2}{2}R_0'^2(\beta_m a). \tag{4.9}$$

Here β_m represents the positive roots of the below expression:

$$\frac{J_0(\beta_m a)}{J_0(\beta_m b)}-\frac{Y_0(\beta_m a)}{Y_0(\beta_m b)}. \tag{4.10}$$

On employing the finite Hankel transform, the BC & IC are modified to:

$$\left[\Upsilon(\beta_m,\tau)\right]_{\bar{r}=\bar{a},\bar{b}} = 0, \tag{4.11}$$

$$\left[\Upsilon(\beta_m,\tau)\right]_{\tau=0} = 0. \tag{4.12}$$

Applying the Laplace transform and then inverse Laplace transform to Eq.(4.6), we obtain:

$$\bar{\Upsilon}(\beta_m,\tau) = \frac{\omega(a^2-b^2)}{2} K_0(\beta_m,\bar{r}) \int_0^{\tau} e^{\left(\frac{\beta_m}{\bar{a}}\right)^2 u} \cos\omega(\tau-u)\,du. \tag{4.13}$$

On applying the inverse Hankel transform to Eq.(4.13), we obtain:

$$\bar{\Upsilon}(\bar{r},\tau) = \frac{\omega(a^2-b^2)}{2} \sum_{m=1}^{\infty} \left\{ K_0^2(\beta_m,\bar{r}) \int_0^{\tau} e^{\left(\frac{\beta_m}{\bar{a}}\right)^2 u} \cos\omega(\tau-u)\,du \right\}. \tag{4.14}$$

Using Eq.(4.14) in Eq.(4.1), we obtain:

$$\bar{H}_z(\bar{r},\tau) = \varphi(\tau) + \frac{\omega\left(a^2-b^2\right)}{2} \sum_{m=1}^{\infty} \left\{ K_0^2(\beta_m,\bar{r}) \int_0^{\tau} e^{\left(\frac{\beta_m}{\bar{a}}\right)^2 u} \cos\omega(\tau-u)\,du \right\}. \tag{4.15}$$

The above equation represents the dimensionless expression for the magnetic field. Further, using Eq.(4.15) in Eq.(2.32) we obtain current density expression in dimensionless form as:

$$\bar{J}_{\theta}(\bar{r},\tau) = -\frac{1}{2\bar{a}}\omega\left(a^2-b^2\right) \left[\sum_{m=1}^{\infty} \left\{ \frac{\frac{\partial}{\partial\bar{r}}\left(K_0^2(\beta_m,\bar{r})\right)}{\left(\frac{\beta_m}{\bar{a}}\right)^4+\omega^2} \left[\left(\frac{\beta_m}{\bar{a}}\right)^2 \left(e^{\left(\frac{\beta_m}{\bar{a}}\right)^2\tau} - \cos\omega\tau \right) + \omega\sin\omega\tau \right] \right\} \right]. \tag{4.16}$$

Using Eq.(4.16) in Eq.(2.33) we obtain the dimensionless expression for eddy current loss as:

$$\bar{w}(\bar{r},\tau) = \frac{\omega^2}{4\bar{a}^2}\left(a^2-b^2\right)^2 \left[\sum_{m=1}^{\infty} \left\{ \frac{\frac{\partial}{\partial\bar{r}}\left(K_0^2(\beta_m,\bar{r})\right)}{\left(\frac{\beta_m}{\bar{a}}\right)^4+\omega^2} \left[\left(\frac{\beta_m}{\bar{a}}\right)^2 \left(e^{\left(\frac{\beta_m}{\bar{a}}\right)^2\tau} - \cos\omega\tau \right) + \omega\sin\omega\tau \right] \right\} \right]^2. \tag{4.17}$$

4.2. Temperature field

Applying the Laplace transform rule to Eqs (2.34) to (2.37), we obtain:

$$\kappa\left[\frac{1}{\bar{r}}\frac{\partial\bar{T}^*}{\partial\bar{r}} + \frac{\partial^2\bar{T}^*}{\partial\bar{r}^2}\right] + \chi_1\bar{w}^* = \chi_2 s\bar{T}^*(\bar{r},s), \tag{4.18}$$

$$\left(\frac{\partial \overline{T}^*}{\partial \overline{r}} + h_b \overline{T}^*\right)_{\overline{r}=1} = 0, \tag{4.19}$$

$$\left(-\frac{\partial \overline{T}^*}{\partial \overline{r}} + h_a \overline{T}^*\right)_{\overline{r}=\overline{a}} = 0, \tag{4.20}$$

$$\left[\overline{T}^*(\overline{r},\tau)\right]_{\tau=0} = 0. \tag{4.21}$$

Applying finite Marchi-Zgrablich integral transform to Eqs (4.18-4.21), we obtain:

$$-\kappa\mu_n^2 \tilde{T}^*(n,s) + \chi_1 \tilde{w}^*(n,s) = \chi_2 \tilde{T}^*(n,s), \tag{4.22}$$

$$\left[\tilde{T}^*(n,s)\right]_{\tau=0} = 0, \tag{4.23}$$

where $\tilde{T}(n,\tau)$ denotes Marchi-Zgrablich transform of $\overline{T}(\overline{r},\tau)$. The transform parameter is denoted by n, and μ_n are the positive roots of the characteristic equation and are read as:

$$J_0(1,\mu a)Y_0(1,\mu b) - J_0(1,\mu b)Y_0(1,\mu a) = 0. \tag{4.24}$$

Applying inverse Laplace transform to Eqs (4.21-4.22), we obtain:

$$\tilde{T}(n,\tau) = \frac{\chi_1}{\chi_2}\int_0^\tau e^{-\left(\frac{\kappa\mu_n^2}{\chi_2}\right)} \tilde{w}(n,\tau-u)du. \tag{4.25}$$

Applying the inverse Marchi-Zgrablich integral transform, we obtain:

$$\overline{T}(\overline{r},\tau) = \sum_{n=1}^{\infty} \frac{\left[\frac{\chi_1}{\chi_2}\int_0^\tau e^{-\left(\frac{\kappa\mu_n^2}{\chi_2}\right)} \tilde{w}(n,\tau-u)du\right] S_p(\alpha,\beta,\mu_n\overline{r})}{\int_a^b \left[\overline{r}\, S_p(\alpha,\beta,\mu_n\overline{r})\right]^2 d\overline{r}}. \tag{4.26}$$

The kernel function $S_p(\alpha,\beta,\mu_n\overline{r})$ can be defined as:

$$S_p(\alpha,\beta,\mu_n\overline{r}) = J_p(\mu_n\overline{r})\left[Y_p(\alpha,\mu_n a) + Y_p(\beta,\mu_n b)\right] - Y_p(\mu_n\overline{r})\left[J_p(\alpha,\mu_n a) + J_p(\beta,\mu_n b)\right], \tag{4.27}$$

where $J_p(\mu\overline{r})$ and $Y_p(\mu\overline{r})$ are the first and second kinds of Bessel's function respectively. Eq.(4.26) represents the dimensionless expression of the temperature field at every instant and all points of the hollow cylinder.

4.3. Elastic field

Neglecting the inertia term from the equation of motion in Eq.(2.42), we obtain:

$$\frac{\partial^2 \overline{u}_r}{\partial \overline{r}^2} + \frac{1}{\overline{r}}\frac{\partial \overline{u}_r}{\partial \overline{r}} - \frac{1}{\overline{r}^2}\overline{u}_r = \chi_3 \frac{\partial T}{\partial \overline{r}} + \frac{\partial}{\partial \overline{r}}(\overline{H}_z)^2. \tag{4.28}$$

Solving Eq.(4.28) and using the boundary conditions given in Eqs (2.43) and (2.44), we obtain:

$$\overline{u}(\overline{r},\tau) = \frac{1}{\overline{r}}\int\left[\chi_3 \overline{r}\,\overline{T} + \overline{r}\left(\overline{H}_z\right)^2 - \overline{r}\left(\varphi(\tau)\right)^2\right]d\overline{r}. \tag{4.29}$$

Using Eq.(4.29) in Eqs (2.39-2.41), we derive the quasi-static stress solutions as follows:

$$\begin{aligned}\overline{\sigma}_{rr}(\overline{r},\tau) &= \frac{1}{\overline{r}}\left[\chi_3 \overline{r}\,\overline{T} + \overline{r}\left(\overline{H}_z\right)^2 - \overline{r}\left(\varphi(\tau)\right)^2\right] - \\ &+ \frac{1}{\overline{r}^2}\left(\frac{1-2\nu}{1-\nu}\right)\int\left[\chi_3 \overline{r}\,\overline{T} + \overline{r}\left(\overline{H}_z\right)^2 - \overline{r}\left(\varphi(\tau)\right)^2\right]d\overline{r} - \chi_3 \overline{T},\end{aligned} \tag{4.30}$$

$$\begin{aligned}\overline{\sigma}_{\theta\theta}(\overline{r},\tau) &= \frac{1-\lambda}{\overline{r}^2}\int\left[\chi_3 \overline{r}\,\overline{T} + \overline{r}\left(\overline{H}_z\right)^2 - \overline{r}\left(\varphi(\tau)\right)^2\right]d\overline{r} + \\ &+ \frac{\lambda}{\overline{r}}\left[\chi_3 \overline{r}\,\overline{T} + \overline{r}\left(\overline{H}_z\right)^2 - \overline{r}\left(\varphi(\tau)\right)^2\right] - \chi_3 \overline{T},\end{aligned} \tag{4.30}$$

$$\begin{aligned}\overline{\sigma}_{zz}(\overline{r},\tau) &= \frac{1}{\overline{r}^2}\left(\frac{1-2\nu}{1-\nu}\right)\int\left[\chi_3 \overline{r}\,\overline{T} + \overline{r}\left(\overline{H}_z\right)^2 - \overline{r}\left(\varphi(\tau)\right)^2\right]d\overline{r} + \\ &+ \frac{1}{\overline{r}}\left(\frac{\nu}{1-\nu}\right)\left[\chi_3 \overline{r}\,\overline{T} + \overline{r}\left(\overline{H}_z\right)^2 - \overline{r}\left(\varphi(\tau)\right)^2\right] - \chi_3 \overline{T}.\end{aligned} \tag{4.31}$$

5. Numerical results and discussion

Figure 1 depicts a conducting hollow circular cylinder composed of aluminum material that is exposed to a time-varying electromagnetic field. The function $\varphi(\tau)$ of time-varying applied magnetic field is defined as follows:

$$\varphi(\tau) = \sin(\omega\tau), \tag{5.1}$$

where $\omega = 2\pi f$ is the angular frequency of the applied magnetic field, which can be calculated from the penetration depth of the field using the decay of one Neper (*0.368*), and is provided by [35]:

$$\delta = \frac{1}{\sqrt{\sigma\mu\pi f}}. \tag{5.2}$$

We perform the numerical calculations for aluminum using the analytical results mentioned above; its material attributes are provided by [5]:

$$\mu_e = 4\pi\times 10^{-7}\ [H/m], \quad \sigma = 4.1\times 10^{7}\ [S/m], \quad \rho = 2702[kg/m^3], \quad E = 72[GPa],$$

$$\nu = 0.3, \quad \alpha = 24\times 10^{-6}\ [K^{-1}], \quad k = 97\times 10^{-6}\ [m^2/s], \quad \lambda = 237[W/(mK)],$$

$$C = 903\ [J/(kgK)], \quad h = 180[W/(m^2K)], \quad \bar{h}_a = \bar{h}_b = 1.0.$$

Also, we fix the outer radius as $b = 0.0001\,(m)$, essential for the convergence of the solution. For illustration purposes, we set the radius ratio $\bar{a} = a/b = 0.2$.

Figure 2 illustrates how skin depth varies with the frequency of electromagnetic waves for different values of magnetic permeability. It demonstrates how skin depth decreases significantly at higher frequencies. Thus, eddy current loss or heating can be controlled to any necessary depth of the conductor by varying the frequency of the supply. Eddy current loss decreases as we go deeper inside the conductor, and it attains the peak value close to the surface due to the phenomenon sometimes known as the "skin effect." It is defined as the uneven propagation of electric current across the surface or skin of the current-carrying conductor. The skin depth δ of the magnetic material defines a certain distance to which the strength of the electromagnetic field suffers the resistance in the amplitude and it reduces to $1/e$ of its original amplitude. This decrease is referred to as the decay of one Naper (0.368).

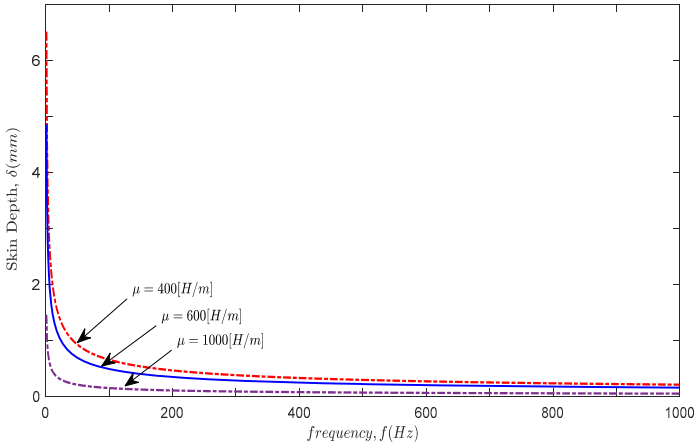

Fig.2. Variation of skin depth with frequency.

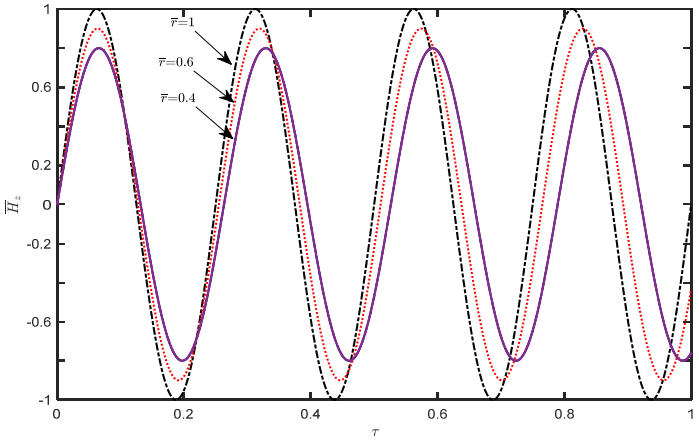

Fig.3. Variation of magnetic field intensity with time.

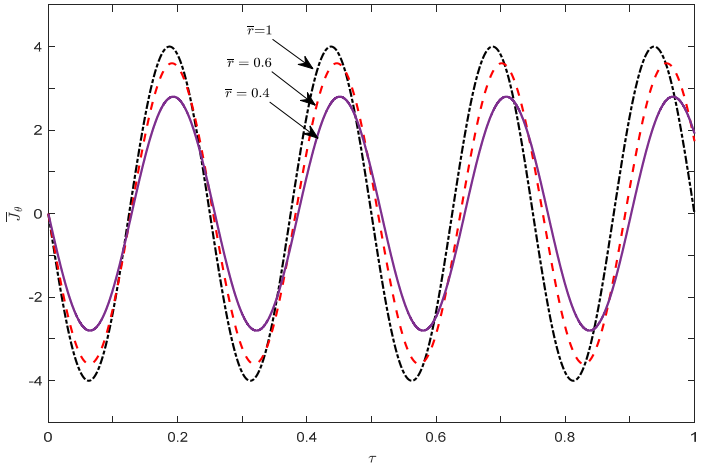

Fig.4. Variation of induced current with time.

Figures 3 and 4 show the time variation of the eddy current $\bar{J}_\theta$ and the magnetic field intensity $\bar{H}_z$ at the innermost surface $(\bar{r} = 0.4)$, inner surface $(\bar{r} = 0.6)$ and at the outer surface $(\bar{r} = 1)$. It can be noticed that these parameters demonstrate the sinusoidal fluctuation with time. This is due to the arbitrary function $\varphi(\tau)$ chosen in terms of sine-profile; see Eq.(5.10).

Figure 5 represents the changes in non-dimensional temperature concerning wave frequency and time. Due to the influence of electromagnetic waves, the cylinder body first heats up, slowly attains the maximum value of temperature, and then moves to a stationary state.

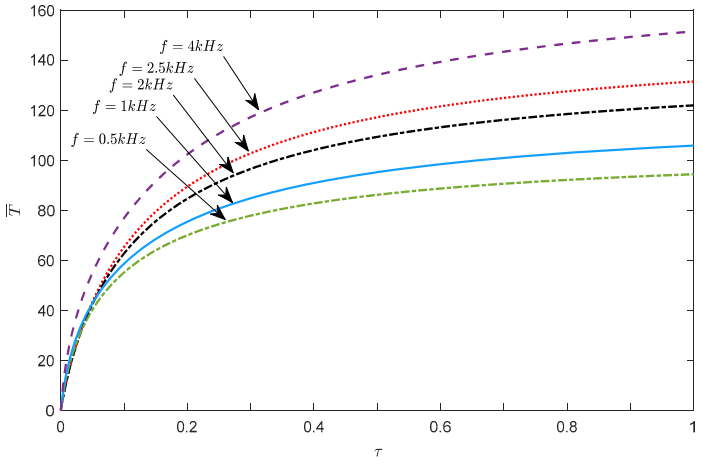

Fig.5. Variation in temperature due to change in time and wave frequency.

Figure 6 shows the time variation of non-dimensional temperature at the innermost surface $(\bar{r} = 0.4)$, inner surface $(\bar{r} = 0.6)$ and at the outer surface $(\bar{r} = 1)$ and it can be seen that the cylinder body heats up gradually at the beginning and attains the maximum temperature then after a few seconds, the temperature moves steadily. It is observed that the temperature is higher at the outer surface as compared to the inner layers This is because, at higher frequencies, the electromagnetic wave can only penetrate near the surface of the conductor material. Therefore, the Joule heating effect is dominant at the outer surface, due to which the temperature of the cylinder is higher at the outer surface. It can also be concluded from this fact that temperature changes always transmit from the surface more slowly compared to eddy currents. Figure 7, demonstrates how the eddy current loss changes with the radius of the cylinder and the frequency of the

electromagnetic field. It can be observed that eddy current loss increases from $(\overline{r}=0)$ to $(\overline{r}=1)$, as the frequency of input supply increases, meanwhile, the magnetic flux density remains constant.

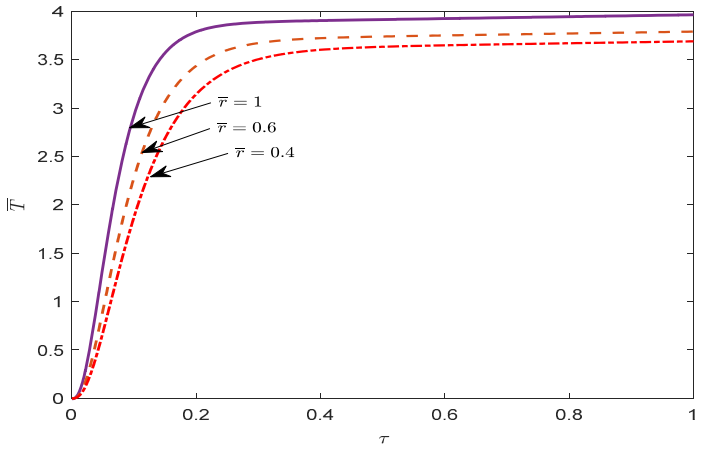

Fig.6. Time variation of non-dimensional temperature.

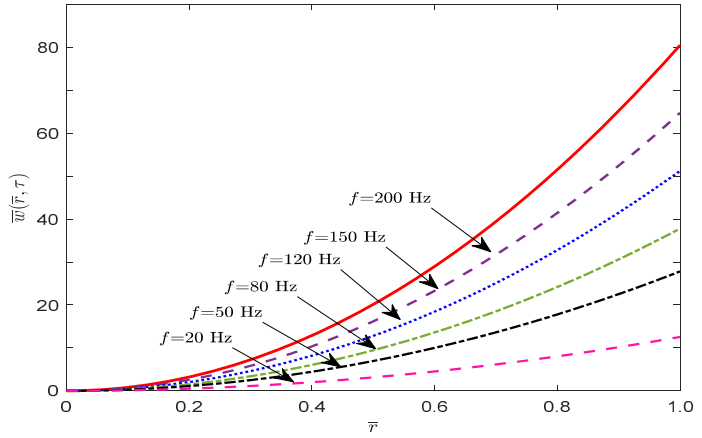

Fig.7. Variation of eddy current loss as a function of radius and frequency.

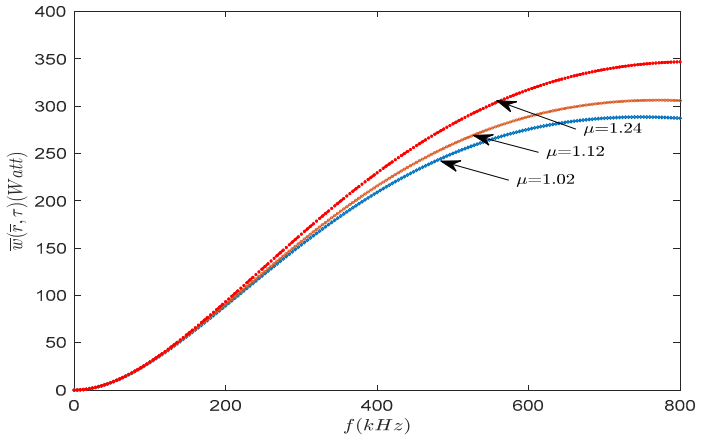

Fig.8. Variation of eddy current loss as a function of magnetic permeability and frequency.

Figure 8 shows the eddy current loss behavior of a hollow circular cylinder for varying magnetic permeability, whereas electrical conductivity is kept constant. It can be seen from the graph that the eddy current loss saturation takes place at higher frequencies because of the lower electrical conductivity. Thus, the effect of losses due to variation in magnetic permeability is observed to be minimal.

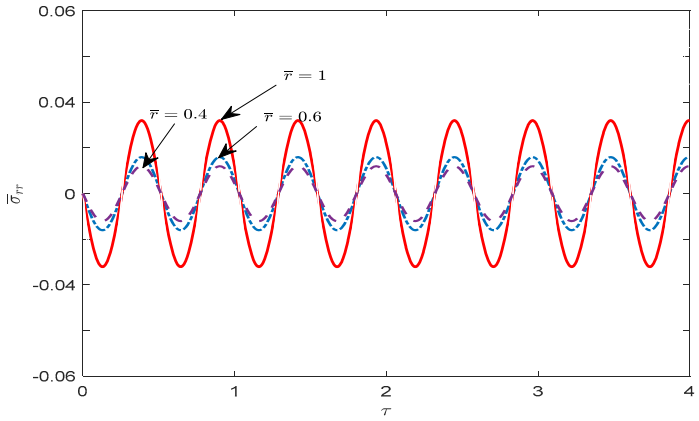

Fig.9. Time variation of radial stress component along the radius of the cylinder.

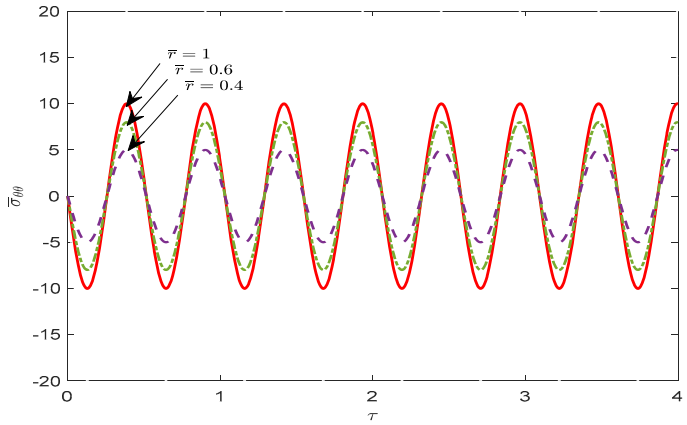

Fig.10. Time variation of circumferential stress component along the radius of the cylinder.

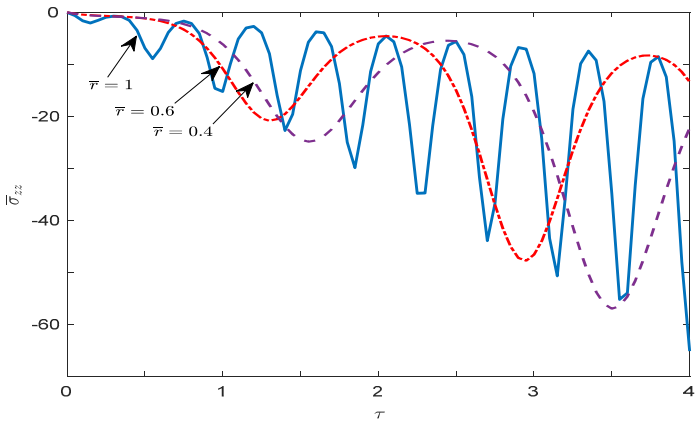

Fig.11. Time variation of axial stress component along the radius of the cylinder.

Figures 9, 10, and 11 show the time variation of quasistatic behavior of the radial stress component $\bar{\sigma}_{rr}$, circumferential stress component $\bar{\sigma}_{\theta\theta}$ and axial stress component $\bar{\sigma}_{zz}$ respectively at the innermost surface $(\bar{r} = 0.4)$, inner surface $(\bar{r} = 0.6)$ and the outer surface $(\bar{r} = 1)$. It can be pointed out that the radial stress amplitudes are substantially less than the circumferential and axial stress amplitudes.

6. Conclusion

In this paper, a one-dimensional problem of magneto-thermo-elasticity under the influence of a time-varying magnetic field is studied. This specific research works with the quasi-static method in uncoupled theory, where the inertia and coupling terms are disregarded in the equation of motion. The problem is described mathematically by Maxwell's equations, and the equations of the magnetic field in terms of a partial differential equation along with the suitable boundary conditions are obtained.

Since problems with inhomogeneous boundary conditions are not very suited for achieving the desired answer in analytical form. In the present article, we have obtained the solutions by using only simple integral transformations (finite Hankel transform, finite Marchi-Zgrablich transform and Laplace transform).

Finite domains play an essential part in real-life applications. Still, due to the intricacy underlying the computations and derivations, relatively limited issues are formulated compared to the infinite domains.

Taking a hollow circular cylinder of aluminum as an example, a series of analyses were carried out. Numerical results of temperature change and stress distributions with the effect of induced eddy current and skin effect are illustrated graphically and are shown in figures with the help of MATLAB software.

It was observed that the time-varying electromagnetic field is responsible for the emergence of conducting currents, which result in the generation of Joule heat. Convection-type barrier on curved parts of a cylinder also impacts the flow of temperature and the stress distribution on headings from inner to outer radii. Skin depth varies inversely with the frequency of electromagnetic waves. Thus, eddy current loss or heating can be customized to any desired depth of the conductor by changing the frequency of the supply. The eddy current loss was found to decrease deeper inside the conductor and was most significant near the surface, which indicated the phenomenon known as the "skin effect."

The suggested study effort in this research paper and the resulting solution to the examined mathematical problem will undoubtedly assist us in the practicality of designing efficient electric machines in multiple fields of engineering in terms of reduced magnetic losses such as eddy current loss.

Acknowledgment

The authors sincerely thank the referees, editorial team members, and Professor Paweł Jurczak, editor-in-chief, for their continuous support and guidance in improving the quality of research work.

Nomenclature

$\vec{B}$ – magnetic flux density
C – specific heat
$\vec{E}$ – electric field intensity
f_r – Lorentz force component
$\vec{H}$ – magnetic field intensity
H_0 – reference magnetic field
h_a, h_b – heat transfer coefficients
$\vec{J}$ – current density
$T(r,t)$ – temperature
u_r, u_θ, u_z – displacement components
$w(r,t)$ – eddy current loss

β – coefficient of linear thermal expansion
δ – skin depth
κ – thermal conductivity
λ,μ – lame's elastic constants
μ_e – magnetic permeability
ν – Poisson ratio
σ – electrical conductivity
$\sigma_{rr},\sigma_{\theta\theta},\sigma_{zz}$ – stress components
ρ – mass density
$\varphi(t)$ – arbitrary function of time
ω – angular frequency

References

[1] Paria G. (1967): *Magneto-elasticity and magneto-thermo-elasticity.*– Advances in Applied Mechanics, vol.10, pp.73-112.

[2] Zhou Y.H. and Zheng X.J. (1999): *Electromagnetic solid structural mechanics*.– Science Press, Peking.

[3] Bai X.Z. (2006): *Magnetic Base Plate and Shell Elasticity*.– Science Press, Peking.

[4] Wang X. (1995): *Thermal shock in a hollow cylinder caused by rapid arbitrary heating.*– Journal of Sound Vibrations,vol.18, pp.899-906.

[5] Xing Y. and Liu B. (2010): *A differential quadrature analysis of dynamic and quasi-static magneto-thermo-elastic stresses in a conducting rectangular plate subjected to an arbitrary variation of magnetic field.*– International Journal of Engineering Science, vol.48, pp.1944-1960. https://doi.org/10.1016/j.ijengsci.2010.06.010

[6] Higuchi M., Kawamura R. and Tanigawa Y. (2007): *Magneto-thermo-elastic stresses induced by a transient magnetic field in a conducting solid circular cylinder*.– International Journal of Solids and Structures, vol.44, No.16, pp.5316-5335.

[7] Higuchi M., Kawamura R. and Tanigawa Y. (2008): *Dynamic and quasi-static behaviors of magneto-thermo-elastic stresses in a conducting hollow circular cylinder subjected to an arbitrary variation of magnetic field.*– International Journal of Mechanical Sciences, vol.50, No.3, pp.365-379, https://doi.org/10.1016/j.ijmecsci.2007.11.001

[8] Moon F.C. and Chattopadhyay S. (1974): *Magnetically induced stress waves in a conducting solid-theory and experiment.*– Journal of Applied Mechanics, Transactions ASME, vol.41, pp.641-646.

[9] Chian C.T. and Moon F.C. (1981): *Magnetically induced cylindrical stress waves in a thermoelastic conductor.*– International Journal of Solids and Structures, vol.17, pp.1021-1035.

[10] Wauer J. (1995): *Parametric vibrations in a magneto-thermo-elastic layer of finite thickness.*– In Proceedings of the 1995 Design Engineering Technical Conferences, vol.3A. New York, ASME, p.407-414.

[11] Pantelyat M.G. and Fe´liachi M. (2002): *Magneto-thermo-elastic-plastic simulation of inductive heating of metals.*– The European Physical Journal Applied Physics, vol.17, No.1, pp.29-33.

[12] Sinha G. and Prabhu S.S. (2011): *Analytical model for estimation of eddy current and power loss in conducting plate and its application.*– Phys, Rev, Accel, Beams, vol.14, p.062401.

[13] Cen S. and Xu J. (2018): *Analysis of thermo-magneto elastic nonlinear dynamic response of shallow conical shells.*– Engineering, vol.10, pp.837-850.

[14] Plotnikov S.M. (2021): *Determination of eddy-current and hysteresis losses in the magnetic circuits of electrical machines.*– Measurement Techniques, vol.63, pp.904-909, DOI:10.1007/s11018-021-01866-9.

[15] Ekergård B. and Leijon M. (2021): *Eddy current losses in solid pole shoes in a two-pole permanent magnet motor.– Engineering*, vol.13, pp.536-543, DOI: 10.4236/eng.2021.1310038.

[16] Wang J.Q., Wang K. and Sun J.R. (2020): *Numerical calculation and test of eddy current loss of magnetic coupling.*– J. Journal of Drainage and Irrigation Machinery Engineering, vol.38, No.03, pp.230-235.

[17] Golebiowski M. (2017): *Calculation of eddy current and hysteresis losses during transient states in laminated magnetic circuits*.– COMPEL - The International Journal for Computation and Mathematics in Electrical and Electronic Engineering, vol.36, No.3, pp.665-682, https://doi.org/10.1108/COMPEL-09-2016-0409.

[18] Kumar N. and Kamdi D.B. (2020): *Thermal behavior of a finite hollow cylinder in the context of fractional thermoelasticity with convection boundary conditions.*– J. Therm. Stress, vol.43, pp.1189-1204.

[19] Lamba N. (2023): *Impact of the memory-dependent response of a thermoelastic thick solid cylinder.*– Journal of Applied and Computational Mechanics, vol.9, No.4, pp.1135-1143, DOI: 10.22055/jacm.2023.43952.4149.

[20] Srinivas V.B., Manthena V.R., Warbhe S.D., Kedar G.D. and Lamba N.K. (2024): *Thermal stresses associated with a thermosensitive multilayered disc analyzed due to point heating.*– International Journal of Applied Mechanics and Engineering, vol.29, No.2, pp.118-137, doi:10.59441/ijame/187051.

[21] Biswas S. (2019): *Eigenvalue approach to a magneto-thermoelastic problem in the transversely isotropic hollow cylinder: comparison of three theories.*– Waves in Random and Complex Media, https://doi.org/10.1080/17455030.2019.1588484

[22] Gao Y., Li K., Wang Y. and He Y. (2016): *Eddy current pulsed thermography with different excitation configurations for metallic material and defect characterization.*– Sensors, vol.16, pp.843, doi:10.3390/s16060843.

[23] Li X., Liu Z., Jiang X., and Lodewijks G. (2016): *Method for detecting damage in carbon-fibre reinforced plastic-steel structures based on eddy current pulsed thermography.*– Nondestructive Testing and Evaluation, vol.33, No.1, pp.1-19, doi:10.1080/10589759.2016.1254213.

[24] Lotfy Kh., El-Bary A. and Tantawi R.S. (2019): *Effects of variable thermal conductivity of a small semiconductor cavity through the fractional order heat-magneto-photothermal theory.*– The European Physical Journal Plus, vol.134, doi:10.1140/epjp/i2019-12631-1.

[25] Abo-Dahab S.M. and Lotfy Kh. (2015): *Generalized magneto-thermoelasticity with fractional derivative heat transfer for a rotation of a fibre-reinforced thermoelastic.*– Journal of Computational and Theoretical Nanoscience, doi:12. 10.1166/jctn.2015.3972.

[26] Lotfy Kh. (2012): *Mode-I crack in a two-dimensional fibre-reinforced generalized thermoelastic problem.*– Chinese Physics B, vol.21, p.014209, doi:10.1088/1674-1056/21/1/014209.

[27] Lotfy Kh. and Tantawi R.S. (2020): *Photo-thermal-elastic interaction in a functionally graded material (FGM) and magnetic field.*– Silicon, vol.12, doi:10.1007/s12633-019-00125-5.

[28] Abo-Dahab S.M., Lotfy Kh. and Gohaly A. (2015): *Rotation and magnetic field effect on surface waves propagation in an elastic layer lying over a generalized thermoelastic diffusive half-space with imperfect boundary.*– Mathematical Problems in Engineering, pp.1-15, doi:10.1155/2015/671783.

[29] Marchi E. and Zgrablich G. (1964): *Vibration in a hollow circular membrane with elastic support*.– Bull. Calcutta Math. Soc., vol.22, No.1, pp.73-76.

[30] Garg M., Rao A. and Kalla S.L. (2007): *On a generalized finite Hankel transform*.– Applied Mathematics and Computation, vol.190, pp.705-711, doi:10.1016/j.amc.2007.01.076.

[31] Sneddon I.N. (1993): *The Use of Integral Transforms*.– McGraw-Hill, New York.

[32] Debnath L. and Bhatta D. (2007): *Integral Transforms and Their Applications*.– second ed., Chapman and Hall/CRC Press, Boca Raton, FL.

[33] Sneddon I.N. (1946): *III. Finite Hankel transforms*.– The London, Edinburgh and Dublin, Philosophical Magazine and Journal of Science: Series 7, vol.37, No.264, pp.17-25, DOI: 10.1080/14786444608521150.

[34] Das P., Kar A. and Kanoria M. (2013): *Analysis of magneto-thermoelastic response in a transversely isotropic hollow cylinder under thermal shock with three-phase-lag effect.*– Journal of Thermal Stresses, vol.36, No.3, pp.239-258, DOI:10.1080/01495739.2013.765180.

[35] Milošević M.V. (2003): *Temperature and stress fields in thin metallic partially fixed plate induced by harmonic electromagnetic wave.*– FME Transactions, vol.31, pp.49-54.

Received: August 2, 2024
Revised: December 30, 2024